EUROPEAN JOURNAL OF BIOMEDICAL AND PHARMACEUTICAL SCIENCES
http://www.ejbps.com

ISSN 2349-8870
Volume: 6
Issue: 2
89-100
Year: 2019

SYNTHESIS OF NEW SPIRO[AZETIDINE-2,3′-INDOLINE]-2′,4-DIONES AS POSSIBLE ANTICANCER AGENTS: *IN VITRO* AND *IN SILICO* STUDIES

Mustapha N. Abubakar[1], José Rubén García-Sánchez[2], Rocio Requena-Castro[3], Francisco Reyes-Espinosa[3], Alfredo Juárez-Saldivar[3], Virgilio Bocanegra-García[3], Gildardo Rivera[3] and Girija S. Singh[1*]

[1]Department of Chemistry, University of Botswana, Private Bag: 0022, Gaborone, Botswana.
[2]Sección de Estudios de Posgrado e Investigación, Escuela Superior de Medicina, Instituto Politécnico Nacional, 11340 Ciudad de México, México.
[3]Laboratorio de Biotecnología Farmacéutica, Centro de Biotecnología Genómica, Instituto Politécnico Nacional, 88710, Reynosa, México.

***Corresponding Author: Girija S. Singh**
Department of Chemistry, University of Botswana, Private Bag: 0022, Gaborone, Botswana.

Article Received on 11/12/2018 **Article Revised on 01/01/2019** **Article Accepted on 22/01/2019**

ABSTRACT

The paper describes the synthesis, and *in vitro* and *in silico* biological evaluation of twelve new spiro[azetidine-2,3′-indoline]-2′,4-diones as possible anti-cancer agents. A series of six compounds have been synthesized by a 1:2 molar reaction of 3-(*N*-substituted)imino-5-chloroisatin with 2-diazo-1,2-diphenylethanone. Treatment of the products with ethanolic sodium hydroxide leads to the formation of a new series of six spiro[azetidine-2,3′-indoline]-2′,4-diones bearing free-NH on 2-oxindole ring. The compounds have been characterized based on analytical and spectral data. The biological evaluation *in vitro* on breast cancer cells (MDA-MB-231 and MCF-7) was performed. Additionally, an *in silico* analysis on active site of MDM2 protein was done to understand potential mechanism of action as anti-cancer agents. The compounds **6a**, **6c** and **6f** exhibited cytotoxic activity (IC_{50} from 2.24 to 22.8 µM) against MDA-MB-231 and MCF-7 cells. Regarding breast cancer cell versus breast normal cells (MCF10A) or normal cells (3T3-L1) **6a**, **6c** and **6f** showed selectivity for growth inhibition of cancerous cells. Molecular docking analysis revealed an equal binding pattern between compound **6a** and compound spiro-oxindole 6SS (a potent MDM2 inhibitor) on active site of MDM2 protein.

KEYWORDS: Spiro-oxindoles, 2-azetidinones, cycloaddition, amide-cleavage, anticancer, MDM2.

GRAPHICAL ABSTRACT

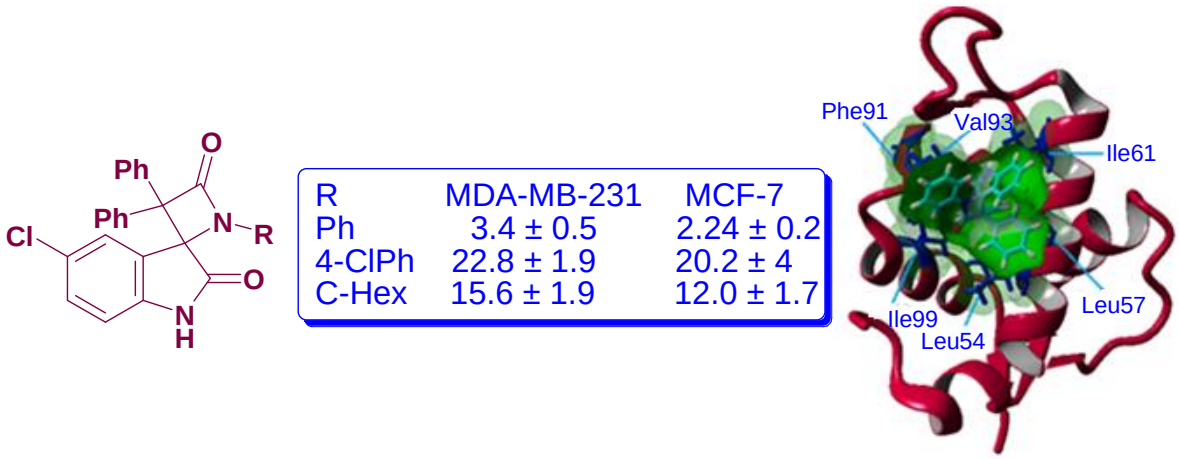

INTRODUCTION

Recent years have seen resurgence of interest in the synthesis of compounds bearing spiro-oxindole motif.[1,2] Spiro-oxindole skeleton occurs in many biologically important alkaloids. Many synthetic spiro-oxindoles have shown different types of biological activities such as anticancer, antibacterial, and antimalarial, among others.[3] Particularly, spiro-oxindoles have been proposed as scaffold to design new potent anticancer agents, suggested that their mechanism of action is through inhibition of MDM2−p53 interaction.[4,5] Especially, spiro-oxindoles bearing a chloro group on 2-oxindole ring have been observed to have significant bioactivity (Fig. 1).[3]

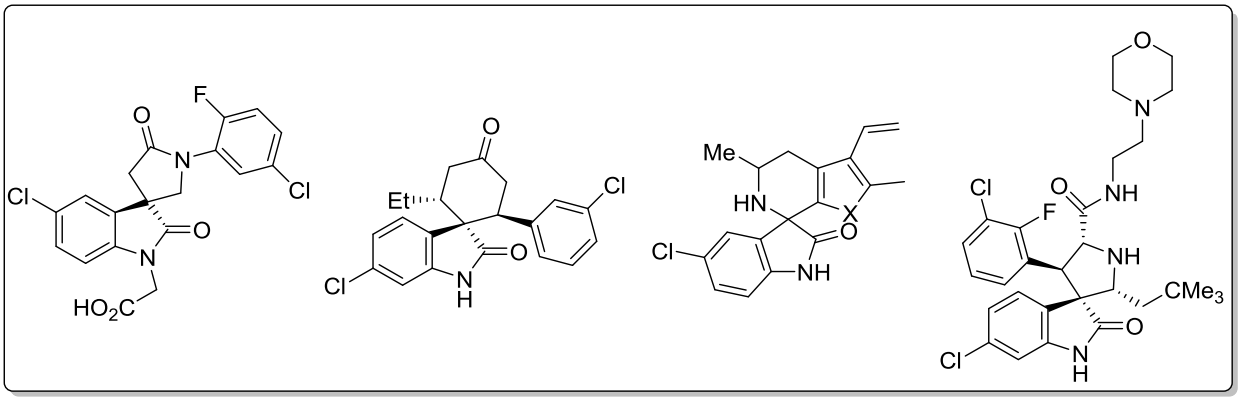

Fig. 1. Some bioactive spirooxindoles containing chloro group on 2-oxindole ring.

On the other hand, compounds containing the β-lactam ring are also well-known in the medicinal and synthetic organic chemistry.[6,7] Besides being potential antibiotics, they are also known to exhibit cholesterol absorption inhibition,[8] and anticancer activity.[9] Since spiro-oxindoles and β-lactams are considered as important scaffolds for development of new potential anticancer agents, our research group considered pertinent to synthesize a molecular framework containing spiro-oxindoles, bearing a chloro group on oxindole ring in particular, and a β-lactam ring to obtain a synergic effect in the bioactivity and evaluate their anticancer activity.

There are many methods known in literature for the synthesis of spiro-oxindoles. Isatin derivatives, however, serve as privileged molecules for the synthesis spiro-oxindole framework.[1] The functional group transformations at C-3 position of isatin constitute a powerful strategy to synthesize spiro-oxindoles. The most common method for constructing the β-lactam ring is the Staudinger's ketene-imine cycloaddition.[7] The ketenes are generated either from acyl chlorides in the presence of an organic base or by thermal/photochemical decomposition of 2-diazocarbonyl compounds. Our group has been using 2-diazo-1,2-diarylketones for generating diarylketenes because this method is simple and does not require any base or activating group.[10,11]

The present paper, thus, reports synthesis of some new 5-chloro-2-oxindoles, spiro-fused to 2-azetidinone ring by the reaction of 3-(*N*-substituted)imino-2-oxindoles with 2-diazo-1,2-diphenylethanone. Spiro-oxindoles with free N-H have been synthesized by selective N-C bond cleavage in the products using ethanolic sodium hydroxide. The biological screening of these compounds has been done on two breast cancer cell lines (MDA-MB-231 and MCF-7) to know their biological effect as anticancer agents. Additionally, the paper also reports the results of an *in silico* study on MDM2 protein as an anticancer target carried out to understand the potential interactions on the active site.

MATERIAL AND METHODS

Chemistry

Melting points have been recorded on a Stuart Scientific melting point apparatus and are uncorrected. The IR spectra were recorded on a Perkin-Elmer-781 IR spectrophotometer using KBr disc of the sample. The ^{1}H and ^{13}C NMR spectra were recorded in a CD_3COCD_3 solution at 300 MHz and 75.4 MHz, respectively, on a Bruker™ 300 MHz spectrometer.

Benzil, 4-chloroisatin, hydrazine hydrate, and amines were Aldrich products. Benzene was dried by refluxing over sodium hydride.

5-Chloroisatin imines **3** were prepared by the condensation of 5-chloroisatin **1** and appropriate amines **2** following the method of Popp and Piccirilli.[12] The 2-diazo-1,2-diphenylethanone **4** was prepared by oxidation of the benzil monohydrazone.[13] The latter compound, in turn, was prepared by the condensation of benzil with hydrazine hydrate by reported method.[14]

Preparation of compounds 5a-f

A solution of 2-diazo-1,2-diphenylethanone **4** (4 mmol) and isatin imines **3** (2 mmol) in 20 mL of dry benzene was heated to reflux under an atmosphere of nitrogen for 6-8 h. The reaction mixture was allowed to stand overnight at room temperature. The solvent was evaporated under reduced pressure using a rotary evaporator. The residue was triturated with ethanol to

afford the white crystalline products 5. The spectral data of the products are given below.

1′-(Diphenylacetyl)-1,3,3-triphenylspiro[azetidine-2,3′-(5′-chloroindoline]-2′,4-dione (5a)

IR (KBr, cm^{-1}): 1762, 1748, 1712; ^1H NMR (CD_3COCD_3, δ ppm): 8.50 (d, 1H, arom), 7.69 (t, 2H, arom), 7.67 – 7.07 (m, 24H, arom), 6.31 (s, 1H, NCO-CH-Ph_2), 6.30 (d, 1H, arom); ^{13}C NMR (CD_3COCD_3, δ ppm): 172.81, 172.13, 165.26, 139.36, 138.55, 138.40, 137.56, 136.83, 135.95, 130.10, 129.44, 129.03, 128.66, 128.62, 128.55, 128.52, 128.32, 128.10, 127.70, 127.35, 127.27, 127.27, 126.69, 126.00, 125.00, 124.22, 118.59, 117.15, 78.70, 71.35, 57.31; MS (m/z, r. i.): 645 (M^+, 8), 451 (M^+-Ph_2C=C=O, 8), 257 (10), 194 (100), 166 (24), 77 (5).

1′-(Diphenylacetyl)-1-(4-methylphenyl)-3,3-diphenylspiro[azetidine-2,3′-(5′-chloroindoline]-2′,4-dione (5b)

IR (KBr, cm^{-1}): 1763, 1756, 1715; ^1H NMR (CD_3COCD_3, δ ppm): 8.49 (d, 1H, arom), 7.69 (d, 2H, arom), 7.67 (t, 1H, arom), 7.36 (m, 22H, arom), 6.31 (s, 1H, NCO-CH-Ph_2), 6.29 (d, 1H, arom), 2.30 (s, 3H, Ph-CH_3); ^{13}C NMR (CD_3COCD_3, δ ppm): 172.92, 172.15, 165.05, 139.37, 138.57, 138.40, 137.65, 136.94, 134.70, 133.48, 130.93, 130.09, 129.81, 129.04, 128.64, 128.60, 128.56, 128.52, 128.28 (two Cs), 128.10, 127.66, 127.35, 127.25, 126.70, 125.99, 124.34, 118.54, 117.28, 78.69, 71.40, 57.27, 19.93; MS (m/z, r. i.): 659 (M^+, 5), 465 (M^+-Ph_2C=C=O, 10), 194 (100), 166 (20), 91 (5).

1′-(Diphenylacetyl)-1-(4-chlorophenyl)-3,3-diphenylspiro[azetidine-2,3′-(5′-chloroindoline]-2′,4-dione (5c)

IR (KBr, cm^{-1}): 1762, 1759, 1714; ^1H NMR (CD_3COCD_3, δ ppm): 8.50 (d, 1H, arom), 7.68 (d, 2H, arom), 7.59 (m, 1H, arom), 7.42 – 7.10 (m, 22H, arom), 6.34 (d, 1H, arom), 6.28 (s, 1H, -CO-CH-Ph_2); ^{13}C NMR (CD_3COCD_3, δ ppm): 172.64, 172.07, 165.34, 139.42, 138.48, 138.43, 137.36, 136.63, 134.72, 131.14, 130.18, 129.60, 129.43, 129.06, 128.70, 128.65, 128.54, 128.40, 128.06, 127.76, 127.37, 127.23, 126.61, 126.07, (123.84, 118.77 two Cs each), 118.68, 79.06, 71.51, 57.35; MS (m/z, r. i.): MS (m/z, r. i.): 680 (M^+, 6), 486 (M^+-Ph_2C=C=O, 10), 194 (100), 166 (30), 110 (8), 78 (2).

1′-(Diphenylacetyl)-1-(4-methoxyphenyl)-3,3-diphenylspiro[azetidine-2,3′-(5′-chloroindoline]-2′,4-dione (5d)

IR (KBr, cm^{-1}): 1769, 1720, 1757; ^1H NMR (CD_3COCD_3, δ ppm): 8.47 (d, 1H, arom), 7.69 (d, 2H, arom), 7.63 (m, 1H, arom), 7.55 – 7.24 (m, 18H, arom), 7.01 (m, 2H, arom), 6.75 (m, 2H, arom), 6.29 (s, 1H, NCO-CH-Ph_2), 6.29 (m, 1H, arom), 3.72 (s, 3H, OMe); ^{13}C NMR (CD_3COCD_3, δ ppm): 173.01, 172.14, 164.89, 157.08, 139.44, 138.56, 138.38, 137.74, 137.04, 130.93, 130.06, 129.43, 129.04, 128.96, 128.62, 128.59, 128.51, 128.26, 128.10, 127.62, 127.34, 127.27, 126.72, 126.02, 124.34, 119.21 (two Cs), 118.49, 114.52, 78.76, 71.61, 57.32, 54.81; MS (m/z, r. i.): 675 (M^+, 5), 481 (20), 450 (15), 287 (50), 194 (100), 165 (40),

1′-(Diphenylacetyl)-1-(4-ethoxyphenyl)-3,3-diphenylspiro[azetidine-2,3′-(5′-chloroindoline]-2′,4-dione (5e)

IR (KBr, cm^{-1}): 1769, 1757, 1706; ^1H NMR (CD_3COCD_3, δ ppm): 8.40 (d, 1H, arom), 7.65 (d, 2H, arom), 7.62 (m, 1H, arom), 7.50 – 7.19 (m, 18H, arom), 7.00 (m, 2H, arom), 6.70 (m, 2H, arom), 6.30 (s, 1H, -CO-CH-Ph_2), 6.28 (m, 1H, arom), 3.92 (q, 2H, OCH_2), 1.30 (t, 3H, CH_3); ^{13}C NMR (CD_3COCD_3, δ ppm): 173.02, 172.15, 164.88, 156.43, 139.44, 138.57, 138.40, 137.75, 137.05, 130.93, 130.08, 129.44, 129.06, 128.85, 128.63, 128.59, 128.52, 128.26, 128.12, 127.64, 127.36, 127.28, 126.73, 126.04, 124.37, (119.22 two C), 118.50, 115.04, 78.77, 71.62, 63.34, 57.32, 14.14; MS (m/z, r. i.): 689 (M^+, 5), 495 (15), 330 (4), 302 (80), 274 (10), 194 (100), 165 (30), 139 (10), 83 (5).

1′-(Diphenylacetyl)-1-cyclohexyl-3,3-diphenylspiro[azetidine-2,3′-(5′-chloroindoline]-2′,4-dione (5f)

IR (KBr, cm-1): 1769, 1755, 1717; ^1H NMR (CD_3COCD_3, δ ppm): 8.34 (d, 1H, arom), 7.40-6.99 (m, 20H, arom), 6.80 (dd, 1H, arom), 6.32 (s, 1H, -CO-CH-Ph_2), 6.28 (m, 1H, arom), 3.19 (m, 1H, N-CH), 2.25 - 2.16 (m, 2H, *C*-hex), 1.70-1.10 (m, 8H, *C*-hex); ^{13}C NMR (CD_3COCD_3, δ ppm): 175.00, 172.65, 167.86, 140.12, 138.20, 138.28, 137.76, 137.28, 134.72, 131.14, 130.18, 129.50, 129.40 129.10, 128.78, 128.44, 128.30 128.06, 127.86, 127.39, 126.75, 126.00, 123.90, 118.75, 116.80, 77.90, 71.80, 57.30, 54.28, 31.80, 30.30, 25.02, 25.00, 24.80; MS (m/z, r. i.): 651 (M^+, 8), 457 (60), 332 (5), 194 (100), 166 (25).

Preparation of compounds 6a-f

A solution of spiro-oxindole **5** (0.1 mmol) and sodium hydroxide (100 mg) in 15 mL of ethanol was refluxed for 4 h.[15] The solvent was evaporated under reduced pressure and the residue was diluted with 20 mL of water. The solution was neutralized with hydrochloric acid and extracted with dichloromethane. The organic fraction was dried over anhydrous magnesium sulphate. The solvent was removed under reduced pressure to get white crystalline product. The spectral data of the products are given below.

1,3,3-Triphenylspiro[azetidine-2,3′-(5′-chloroindoline]-2′,4-dione (6a)

IR (KBr, cm^{-1}): IR (KBr, cm^{-1}): 3225, 1759, 1727; ^1H NMR (CD_3COCD_3, δ ppm): 10.15 (s, 1H, N-H), 7.60 (m, 2H, arom), 7.35-7.10 (m, 12H, arom), 7.00 (m, 1H, arom), 6.60 (m, 3H, arom); ^{13}C NMR (CD_3COCD_3, δ ppm): 172.90, 167.90, 150.05, 140.50, 140.00, 138.96, 130.30, 129.25, 128.60, 128.20, 128.10, 127.70, 127.48, 127.00, 126.65, 124.75, 122.70, 122.32, 117.20, 110.85, 76.40, 71.52; MS (m/z, r. i.): 451 (M^+, 15), 257 (25), 194 (100), 165 (35), 77 (10).

1-(4-Methylphenyl)-3,3-diphenylspiro[azetidine-2,3′-(5′-chloroindoline]-2′,4-dione (6b)

IR (KBr, cm^{-1}): 3245, 1753, 1724; ^1H NMR (CD_3COCD_3, δ ppm): 10.07 (s, 1H, N-H), 8.04 (s, 4H, arom), 7.43 (m, 5H, arom), 7.05 (m, 5H, arom), 6.61 (d, 3H, arom), 2.43 (s, 3H, Ph-CH_3); ^{13}C NMR (CD_3COCD_3, δ ppm): 173.10, 167.80, 150.30, 140.38, 140.00, 138.85, 134.10, 130.03, 128.46, 128.35, 128.00, 127.53, 127.65, 127.21, 126.55, 124.45, 122.38, 122.18, 117.43, 76.35, 71.67, 19.93; MS (m/z, r. i.): 465 (M^+, 12), 271 (30), 194 (100), 165 (35), 91 (10).

1-(4-Chlorophenyl)-3,3-diphenylspiro[azetidine-2,3′-(5′-chloroindoline]-2′,4-dione (6c)

IR (KBr, cm^{-1}): IR (KBr, cm^{-1}): 3241, 1752, 1717; ^1H NMR (CD_3COCD_3, δ ppm): 10.04 (s, 1H, N-H), 8.04 (d, 1H, arom), 7.62 – 7.50 (m, 5H, arom), 7.46 – 7.35 (m, 4H, arom), 7.15 – 7.00 (m, 6H, arom), 6.57 (d, 1H, arom): ^{13}C NMR (CD_3COCD_3, δ ppm): 174.65, 166.78, 149.28, 145.86, 133.96, 133.60, (129.71, 128.32 two C each), 126.27, (125.31, 122.55 two C each), 121.19, (119.23, 117.13 two C each), 78.75, 72.06; MS (m/z, r. i.): 485 (M^+, 8), 291 (20), 194 (100), 165 (30), 111 (5).

1-(4-Methoxyphenyl)-3,3-diphenylspiro[azetidine-2,3′-(5′-chloroindoline]-2′,4-dione (6d)

IR (KBr, cm^{-1}): 3244, 1750, 1723; ^1H NMR (CD_3COCD_3, δ ppm): 10.07 (s, 1H, N-H), 8.00 (d, 1H, arom), 7.55 (d, 2H, arom), 7.42 (m, 1H, arom), 7.50 – 7.29 (m, 8H, arom), 6.80 (m, 2H, arom), 6.60 (m, 2H, arom), 6.29 (m, 1H, arom), 3.69 (s, 3H, OMe); ^{13}C NMR (CD_3COCD_3, δ ppm): 172.10, 167.56, 157.35, 149.60, 140.75, 138.30, 137.80, 130.65, 130.24, 128.75, 128.40, 128.00, 127.82, 127.45, 127.00, 122.95, 122.45, 119.00, 115.24, 79.06, 71.51. 57.24; MS (m/z, r. i.): 481 (M^+, 10), 287 (30), 194 (100), 165 (38), 107 (5).

1-(4-Ethoxyphenyl)-3,3-diphenylspiro[azetidine-2,3′-(5′-chloroindoline]-2′,4-dione (6e)

IR (KBr, cm^{-1}): 3248, 1754, 1728; ^1H NMR (CD_3COCD_3, δ ppm): 10.07 (s, 1H, N-H), 8.38 (d, 1H, arom), 7.58 (d, 2H, arom), 7.40 – 7.10 (m, 10H, arom), 6.85 (m, 2H, arom), 6.70 (m, 1H, arom), 6.20 (m, 1H, arom), 3.85 (q, 2H, OCH_2), 1.34 (t, 3H, CH_3); ^{13}C NMR (CD_3COCD_3, δ ppm): 173.32, 167.28, 156.74, 140.57, 138.30, 137.85, 130.35, 129.95, 120.30, 128.15, 128.00, 127.95, 127.69, 127.25, 126.75, 122.65, 122.10, 119.30, 114.85, 111.22, 78.75, 71.40, 62.80, 14.28; MS (m/z, r. i.): 495 (M^+, 10), 301 (25), 194 (100), 165 (20).

1-Cyclohexyl-3,3-diphenylspiro[azetidine-2,3′-(5′-chloroindoline]-2′,4-dione (6f)

IR (KBr, cm-1): 3190, 1756, 1728; ^1H NMR (CD_3COCD_3, δ ppm): 10.08 (s, 1H, N-H), 7.55 (d, 2H, arom), 7.35 – 7.10 (m, 8H, arom), 6.88 (d, 1H, arom), 6.70 (m, 1H, arom), 6.18 (m, 1H, arom), 3.34 (m, 1H, N-CH), 2.25-2.10 (m, 2H, *C*-hex)), 1.65-1.18 (m, 8H, *C*-hex); ^{13}C NMR (CD_3COCD_3, δ ppm): 174.56, 168.68, 140.58, 138.63, 134.35, 130.00, 128.25, 128.16, 128.00, 127.24, 127.00, 126.90, 126.76, 124.18, 110.95, 79.15, 72.75, 54.25, 31.75, 30.36, 25.10, 25.05, 24.90; MS (m/z, r. i.): 457 (M^+, 12), 263 (100), 194 (80), 181 (15) 166 (35), 118 (10), 55 (5).

Biology

Cell cultures

The cell lines used in this study MDA-MB-231, MCF-7, MCF-10A and 3T3-L1 were obtained from the American Type Culture Collection (ATCC), (Manassas, Virginia, USA). MDA-MB-231 and MCF-7 breast cancer cells were grown in DMEM high glucose, supplemented with 5% fetal bovine serum (FBS, Atlanta Biological). The non-tumorigenic mammary epithelial cells MCF10A were grown in DMEM/F12 media, supplemented with 5% horse serum, 0.5 µg hydrocortisone, 20 ng/mL EGF and 10 µg/mL insulin while fibroblast cells (3T3-L1) were grown in DMEM high glucose supplemented with 10% bovine calf serum. All the media (Gibco Lab, USA) were also supplemented with 2 mM glutamine, 100 U/mL penicillin and 100 mg/mL streptomycin. The cells were maintained in a humidified incubator at 37 °C with 5% CO_2 and 95% air.

Cell viability assays

Each cell line was seeded at 1×10^4 cells in 96-well tissue culture plates, allowed to attach in incubation for 24 h before the test. The cells were then treated with different concentrations of **6a** (1-5 µM), **6c** (5-35 µM) and **6f** (10-30 µM). The compounds were dissolved in DMSO, negative control contained DMSO was also evaluated and each concentration was performed in quadruplicate, in three different experiments. All culture on microplates with the treatments were incubated at 37 °C under humid atmosphere with 5% CO_2 for 72 h, then the MTT (final concentration 3 mg/mL) was added and incubated for 2.5 h (Mosman 1983). After discarding the medium, 200 µL of DMSO was applied to each well to dissolve the dark-blue formazan crystals in intact cells, and the resulting solution was measured by spectrophotometry with the microplate reader (The synergy HT, BioTek) at a wavelength of 550 nm. The results are expressed as the percentage of viability cells in relation to the negative control, whose viability was designated as 100%. The IC_{50} values were calculated by testing different drug concentration- responses and through a logarithmic analysis of four variables using Prism 6 software (GraphPad, San Diego, CA, USA).

***In silico* analysis**

Protein and ligands preparation

The crystal structure of receptor MDM2 binding with spiro-oxindole inhibitor (known as 6SS and named as (3~{S},3'~{S},4'~{S},5'~{S})-4'-azanyl-6-chloranyl-3'-(3-chloranyl-2-fluoranyl-phenyl)-1'-[(3-ethoxyphenyl)methyl]-5'-methyl-spiro[1~{H}-indole-3,2'-pyrrolidine]-2-one), dihydroisoquinolinone inhibitor (known as 4SS and named as (S)-2-(2-((2H-tetrazol-5-yl)methoxy)-4-methylphenyl)-1-(4-chlorophenyl)-6,7-diethoxy-1,2-dihydroisoquinolin-3(4H)-one) and p53 inhibitor (PDB ids: 5LAY, 4ZYC and 1T4F,

respectively) were downloaded from RCSB PDB (www.rcsb.org).[16] All structures were refined by subtracting water molecules. An energy minimization was performed using the YASARA force field.[17] Before performing the docking calculations, the binding sites were analyzed in MDM2 protein with DoGSiteScorer (Suppl. Text S1).

The 3D ligands structure of the two spiro[azetidine-2,3′-indoline]-2′,4-diones series were all constructed from their respective 2D drug molecules with ACD/ChemSketch program.

Docking protocols

The Autodock 4.2 Release 4.2.6 program installed in 3.4 GHz Intel Core i7 processor and 23.5 GB RAM, having Linux Mint 17.3 as operating system, was utilized to perform automated docking studies to predict the MDM2 protein–ligand interaction.[18] All the data files for ligands and receptor MDM2 protein were then saved in PDBQT Format using AutoDockTools program. The receptor was obtained from MDM2–4SS complex (PDB ID: 4ZYC Chain A) and prepared using the DockPrep structure editing tool from UCSF Chimera. Once the receptor was opened in AutoDockTools, the PDBQT file was generated automatically. Grid Box was defined using receptor and 4SS ligand from MDM2 complex. Both spiro-compounds series were evaluated in s1 and s2 site (Suppl. Text S1), one is located in α-helix motif and the other interface, respectively. The grid size in each site was set as X = 40, Y = 40 and Z = 40 pts with a spacing of 0.375 Å and their respective center coordinates were for s1site X = 3.099, Y = -27.400 and Z = 10.716 and for s2 site X = -7.731, Y = -17.411 and Z = 1.860. Affinity maps were generated using AutoGrid4 and the atom types were extracted by screening all PDBQT ligand files. Docking parameter files were developed using AutoDockTools and Docking was performed using Autodock4.[19] The interaction between MDM2 amino acids residues and spiro-compounds on the binding sites was analyzed using PLIP (Protein–Ligand Interaction Profiler) severand LigPlot+ program.[20,19]

Analysis of MDM2–inhibitors complexes interactions

The interactions of MDM2–p53 (PDB: 1T4F), MDM2–6SS (PDB: 5LAY) and MDM2–4SS (PDB: 4ZYC) were analyzed using the scoring function of Autodock. Therefore, the Autodock program was used to evaluate those complexes by editing the Docking procedure and performer the command epdb, according to Autodock scripts.

RESULTS AND DISCUSSION

Chemistry

An equimolar reaction of 5-chloroisatin **1** with amines **2** in ethanol at reflux temperature led to the formation of 3-(*N*-substituted)imino-5-chloroisatins **3** (Scheme 1). Unlike the reaction of unsubstituted isatin with amines as reported by Popp and Piccirilli that required only 30 min for complete conversion of isatin to imines.[12] we would like to mention that the reaction of 5-chloroisatin with amines took 6-8 h for complete conversion to imines.

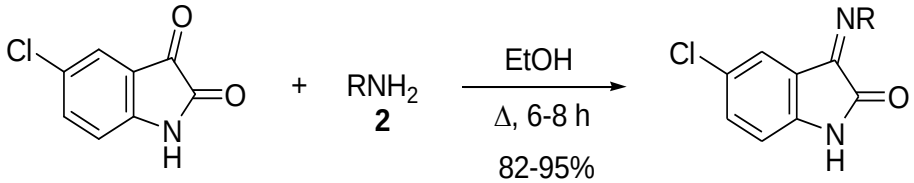

1 **3**

Scheme 1. Synthesis of 3-(N-substituted)imino-5-chloroisatin derivatives.

A 2:1 molar reaction of 2-diazo1,2-diphenylethanone **4** with 3-(*N*-phenylimino)isatin imine **3a** in dry benzene and usual workup afforded a white crystalline compound that has been characterized as 1′-(Diphenylacetyl)-1,3,3-triphenylspiro[azetidine-2,3′-(5′-chloroindoline]-2′,4-dione **5a** on the basis of analytical (Table **1**) and spectral (IR, ^{1}H and ^{13}C NMR, and MS) data (see Material and Method). A similar reaction of isatin imines **3b-f** also yielded the corresponding spiro-oxindole-azetidinones **5b-f** in very good yields (Scheme 2).

Treatment of products **5a-f** with ethanolic sodium hydroxide yielded a new series of spiro-oxindole-azetidinones **6a-f** with free N-H in 2-oxindole ring (Scheme 2) that have been characterized based on satisfactory analytical (Table 1) and spectral data (see Material and Method).

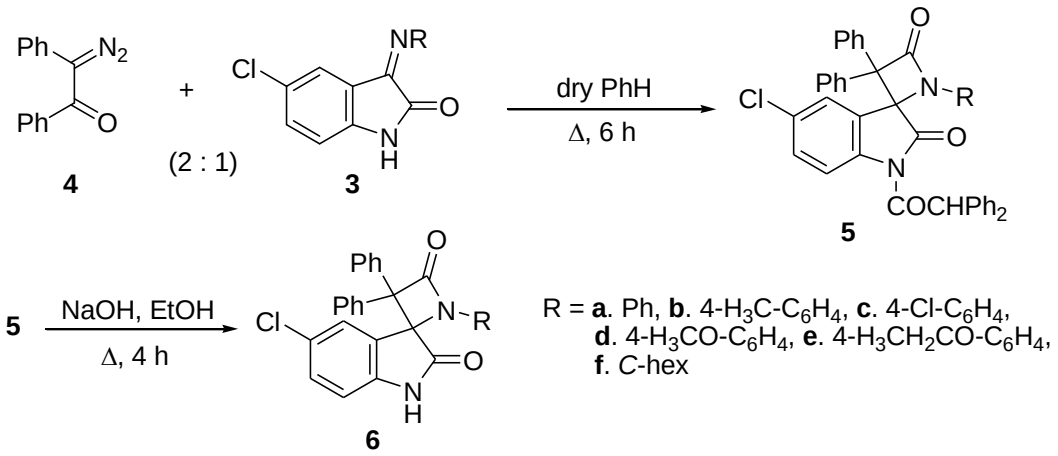

Scheme 2. Route of synthesis of new spiro[azetidine-2,3′-indoline]-2′,4-diones.

Table 1: Physical data of spirooxindoles.

Compd. No.	R	Mol. Formula*	m. p. (°C)	Yields (%)
5a	Ph	$C_{42}H_{29}ClN_2O_3$	120-122	69
5b	4-Me-C_6H_4	$C_{43}H_{31}ClN_2O_3$	208-210	76
5c	4-Cl-C_6H_4	$C_{42}H_{28}Cl_2N_2O_3$	138-140	80
5d	4-MeO-C_6H_4	$C_{43}H_{31}ClN_2O_4$	165-166	79
5e	4-EtO-C_6H_4	$C_{44}H_{33}ClN_2O_4$	201-204	63
5f	*C*-hex	$C_{42}H_{35}ClN_2O_3$	238-240	75
6a	Ph	$C_{28}H_{19}ClN_2O_2$	248-250	98
6b	4-Me-C_6H_4	$C_{29}H_{21}ClN_2O_2$	172-178	99
6c	4-Cl-C_6H_4	$C_{28}H_{18}Cl_2N_2O_2$	134-135	97
6d	4-MeO-C_6H_4	$C_{29}H_{21}ClN_2O_3$	134-136	96
6e	4-EtO-C_6H_4	$C_{30}H_{23}ClN_2O_3$	142-144	96
6f	*C*-hex	$C_{28}H_{25}ClN_2O_2$	218-220	99

*All products showed elemental analyses for C, H, and N in the range of ± 0.4.

Popp and Piccirilli had reported the reaction of unsubstituted isatin with amines taking only 30 min for complete conversion of isatin to imines.[12] We would like to mention, however, that the reaction of 5-chloroisatin with amines took 6-8 h for complete conversion to imines.

The IR spectra of **5a** showed the disappearance of the bands corresponding to N-H and C=N and appearance of additional bands corresponding to carbonyl bonds at 1748 and 1712 cm^{-1}. The ^1H NMR spectra showed a singlet at δ 6.31 ppm besides the required signals for aromatic protons. The ^{13}C NMR spectra showed three downfield signals at δ 172.81, 172.13, and 165.26 corresponding to three carbonyl carbon nuclei in the molecule. The three upfield signals at δ 78.70, 71.35, and 57.31 ppm have been assigned to spiro-carbon, C-3 and methine carbon, respectively. The mass spectra showed the molecular ion peak [M^+] at m/z 644.

The reaction was carried out by taking 2:1 molar ratio of the diazoketone and isatin imines because it was observed earlier that the diphenylketene reacted preferentially with the N-H of isatin imines and not with the 3-imino group.

The IR spectra of 6a-f showed the band corresponding to N-H bond at around 3240 cm^{-1}. The ^1H NMR also showed a broad singlet signal at δ 8.50 (D_2O exchangeable) corresponding to NH proton. The ^{13}C NMR spectra showed only two downfield signals corresponding to two carbonyl carbon nuclei instead of three as observed in 5a-f.

Thermal decomposition of 2-diazo-1,2-diphenylethanone 4 is known to generate benzoylphenylcarbene A that undergoes the Wolff-rearrangement forming diphenylketene B (Scheme 3). The reaction of diphenylketene B at amido nitrogen of isatin imines 3 led to the formation of *zwitterionic* intermediate C that affords 1-diphenylacyl-5-chloro-3-(*N*-substituted)imino-2-oxindoles D. The reaction of a second mole of diphenylketene B with imino group of imines D leads to the formation of a *zwitterionic* intermediate E that cyclizes to give products. Treatment of these compounds with ethanolic sodium hydroxide led to cleavage of *N*-$COCHPh_2$ bond resulting into *N*-deacylation forming products 6a-f.

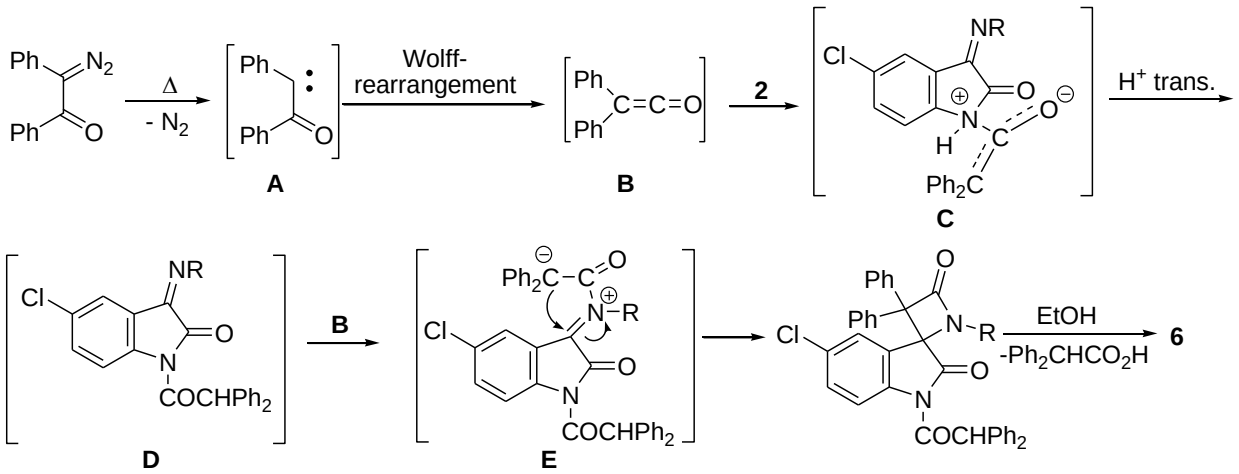

Scheme 3. Mechanism of formation of spiro[azetidine-2,3′-indoline]-2′,4-diones.

Biology

Of the eight compounds screened, only compounds **6a**, **6c** and **6f** showed good solubility for *in vitro* test on cancer cells lines (Fig. 2, Table 2). Concentration response curves were constructed and the percentage of cell viability on breast cancer cells (MDA-MB-231 and MCF-7) and non-cancerous cells (MCF-10A and 3T3-L) was established.

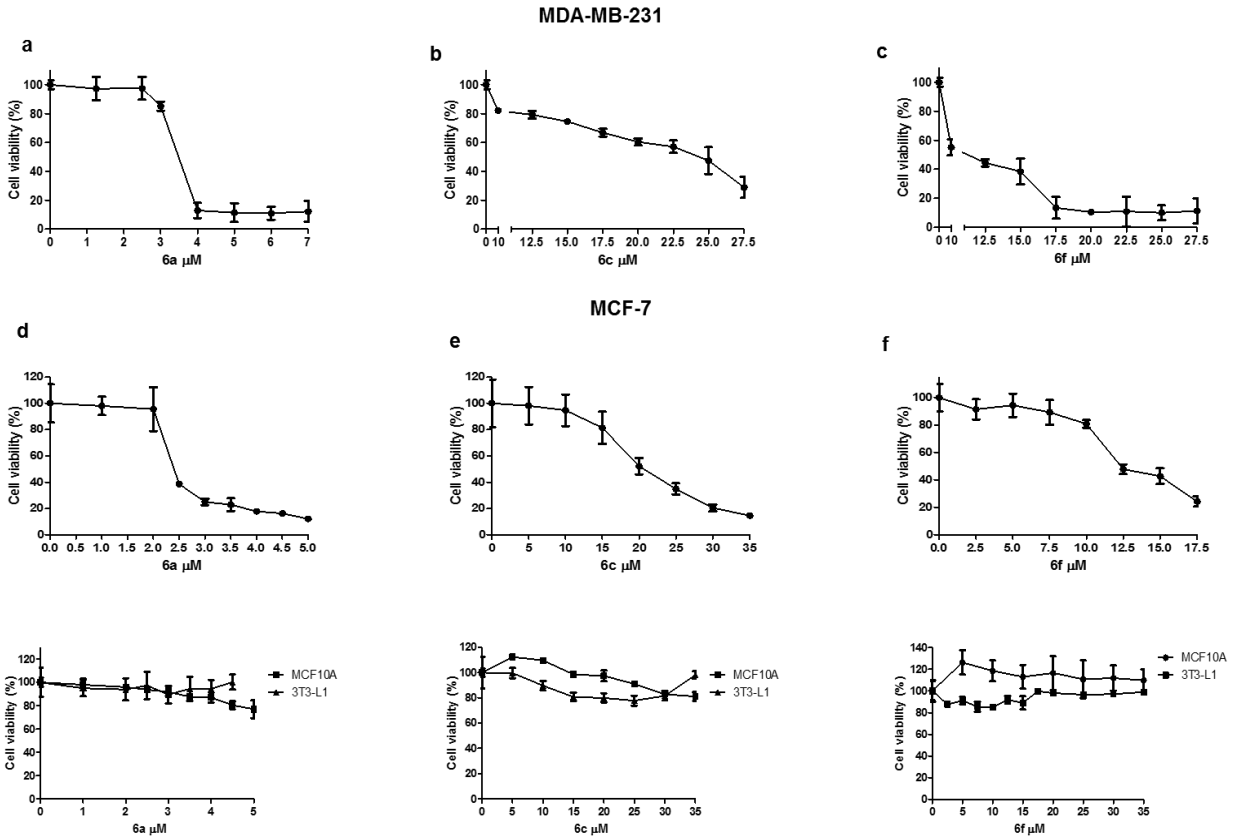

Fig. 2: Percentage of cell viability of compounds 6a, 6c and 6f on breast cancer cells (MDA-MB-231 and MCF-7) and non-cancerous cells (MCF-10A and 3T3-L1).

The calculation of the half maximal inhibitory concentration (IC_{50}) of the compounds was determinated (**Table 2**).

Table 2: Cytotoxic activity (IC_{50} in µM) of spiro-oxindole-azetidinones derivatives in two breast cancer cell lines and non-cancerous cells.

Compds.	MDA-MB-231	MCF-7	MCF10A	3T3-L1
6a	3.4 ± 0.5	2.24 ± 0.2	No effect	No effect
6c	22.8 ± 1.9	20.2 ± 4	No effect	No effect
6f	15.6 ± 1.9	12.0 ± 1.7	No effect	No effect

***In silico* binding prediction**

Spiro-oxindoles have been described as MDM2−p53 interaction inhibitors.[3] It was, therefore, considered pertinent to analyze the interactions in the crystal structure between p53 and MDM2 (PDB: 1T4F) and their two reported inhibitors: spiro-oxindole (**6SS**) and dihydroisoquinolinone (**4SS**) PDB: 5LAY and 4ZYC, respectively (Fig. 3). We detected homologous structures with one and two binding sites, which were employed to prepare *in silico* experiments.

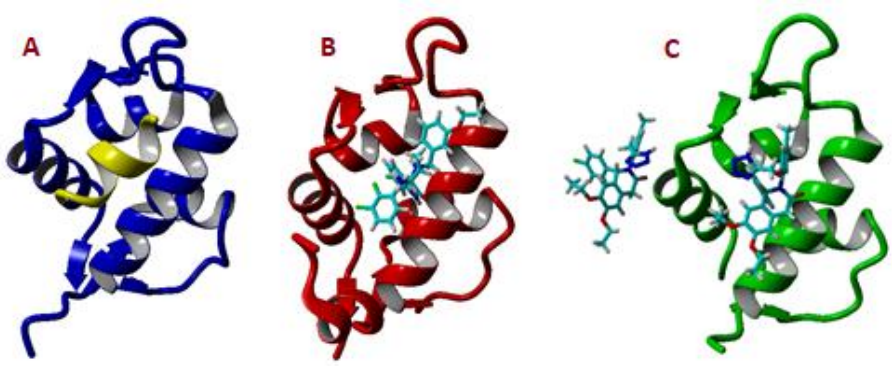

Fig. 3. Structure of the MDM2−inhibitors complexes: A. MDM2−p53 (PDB: 1T4F); B. MDM2−6SS (PDB: 5LAY); C. MDM2−4SS (PDB: 4ZYC)

Binding sites in MDM2 protein (PDB 5LAY) were identified by druggability prediction with DoGSiteScorer (Fig. 4).[21] This analysis was performed on the protein structure of MDM2–**6SS** complex. *In silico* analysis detected two binding sites in MDM2 (Suppl. Text. S1). DoGSiteScorer predicted an average score of 0.6 for a druggable pocket, therefore s1 site is a druggable site. In the case of s2, this site could be a difficult or undruggable site.

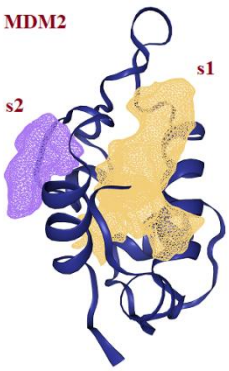

Fig. 4. Binding sites prediction in MDM2 protein.

Once those active sites were identified, the analyses of both series of spiro-oxindole derivatives were performed on MDM2 enzyme. The Docking results were analyzed according the lowest-scoring conformation in free binding energy (ΔG_b) recorded (Table 3), in addition the ΔG_b of the crystallographic models (1T4F, 5LAY and 4ZYC) were analyzed with PDBePISA server (http://www.ebi.ac.uk/msd-srv/prot_int/pistart.html).The structure of the lowest-scoring conformation of each model was analyzed with PLIP sever.[20] Also, an analysis of interactions from series 5 and 6 on active site s1 and s2 was done from results of the PLIP server (Tables 4 and 5) and its respective 2D ligand−protein interaction diagrams performed with LigPlot+ program is presented in Text S2 (Suppl.).[19] The predicted ΔG_b from the crystallographic models showed (Table **3**) a record of ΔG_b lower in MDM2-6SS complex (PDB 5LAY) than in MDM2-p53 complex (PDB 1T4F) the latter being equal in MDM2-4SS complex (PDB 4ZYC), typical characteristic of a competitive inhibitor.

Table 3- Predicted binding energy (ΔG_b) and inhibition constant (K_i). In parenthesis, ΔG_b values calculated from PDB (1T4F, 5LAY and 4ZYC, respectively) and analyzed with PDBePISA server; [£], ΔG_b values calculated during Molecular Docking; [*] Calculated from ΔG_b[£]; [a, b,] and [c], models obtained from PDB 1T4F, 5LAY and 4ZYC, respectively; 6SS, Spiro-oxindole inhibitor; 4SS, dihydroisoquinolinone inhibitor.

Ligand	Site 1		Site 2	
	ΔG_b[£] (kcal/mol)	K_i[*] (µM)	ΔG_b[£] (kcal/mol)	K_i[*] (mM)
p53[a]	(-11.5)			
6SS[b]	-9.83 (-13.5)	0.06		
4SS[c]	-11.03 (-11.1)	0.01	-6.83	0.01
5a	-9.33	0.15	-4.31	0.69
5b	-9.62	0.09	-4.63	0.41
5c	-9.25	0.17	-4.27	0.74
5d	-9.24	0.17	-3.99	1.20
5e	-9.24	0.17	-4.11	0.97
5f	-9.91	0.05	-5.13	0.18
6a	-7.60	2.69	-4.50	0.50
6b	-7.68	2.36	-4.66	0.38
6c	-7.91	1.59	-4.54	0.47
6d	-7.61	2.66	-4.40	0.60
6e	-7.55	2.91	-4.47	0.53
6f	-8.17	1.03	-4.88	0.27

Table 4 Pattern of observed interactions observed of the structure of inhibitors binding to MDM2 protein evaluated in s1 site. I^{Hy}, Hydrophobic interaction; B^{Hy}, Hydrogen bond; Ligands: 6SS, 4SS, 5a, 5b, 5c, 5d, 5e, 5f, 6a, 6b, 6c, 6d, 6e and 6f. Data obtained from results of the PLIP server.

Residue	6SS		4SS	5a	5b		5c		5d		5e		5f		6a	6b		6c			6d			6e			6f		
	I^{Hy}	B^{Ha}	I^{Hy}	I^{Hy}	I^{Hy}	π^S	I^{Hy}	π^S	I^{Hy}	π^S	I^{Hy}	π^S	I^{Hy}	π^S	I^{Hy}	I^{Hy}	π^S	I^{Hy}	π^S	B^{Ha}	I^{Hy}	π^C	B^{Hy}	I^{Hy}	π^S	B^{Ha}	I^{Hy}	π^S	B^{Hy}
Lys[51]			1																										
Leu[54]	2		3	2	2		1		2		1		2		1			2									1		
Phe[55]				2							1							1			1								
Leu[57]	1		1		1		1		1		1		1		1			1			1						1		
Ile[61]	2			1	1		2		2		2		2		1	1		1			1			1			1		
Tyr[67]	1				1	1	1	1	1	1	1	1	1	1															
Gln[72]											1																		
His[73]																							1						
Phe[86]					1		2		2		1		1																
Phe[91]	1				1		1		1		1		1		2												1		
Val[93]	1		2		3		3		2		3		2		2	2		1			2			2					
Lys[94]																								1					
His[96]		1		1													1		1	1		1			1	1		1	1
Arg[97]																													
Lys[98]																													
Ile[99]	1		1	1	1		2		2		2		2		1									2					
Ile[103]							1																						

Table 5- Pattern of observed interactions observed of the structure of inhibitors binding to MDM2 protein evaluated in s2 site. I^{Hy}, Hydrophobic interaction; B^{Hy}, Hydrogen bond; Ligands: 6SS, 4SS, 5a, 5b, 5c, 5d, 5e, 5f, 6a, 6b, 6c, 6d, 6e and 6f. Data obtained from results of the PLIP server.

Residue	4SS		5a	5b		5c		5d		5e		5f		6a		6b		6c		6d		6e		6f	
	I^{Hy}	B^{Hy}	I^{Hy}	I^{Hy}	B^{Hy}	I^{Hy}	B^{Hy}	I^{Hy}	B^{Hy}	I^{Hy}	B^{Hy}	I^{Hy}	B^{Hy}	I^{Hy}	B^{Hy}	I^{Hy}	B^{Hy}	I^{Hy}	B^{Hy}	I^{Hy}	B^{Hy}	I^{Hy}	B^{Hy}	I^{Hy}	B^{Hy}
Gln^{18}														1									1		
Glu^{95}			1					1						1	1	1				1		1			
Arg^{97}	1	2	1	1		1		1		1				1	1	2	1			2		1			
Lys^{98}	1	1	1	2		2		1	1	1		2			1	2	1	1		2				1	
Ile^{99}																									
Thr^{101}		1	1	1	1	1	1	1	1	1	1	1	1			1		1	1		1	1	2	1	1
Arg^{105}									1		1														

The compound **6a** bearing a phenyl group on azetidinone ring exhibited highest activity in both breast cancer cell lines (Figs. 2a and 2d), followed by the compound **6f** (Figs. 2c and 2f) and compound **6c** (Figs 2b and 2e) bearing a cyclohexyl group and a 4-chlorophenyl group, respectively, on azetidinone ring. When the cytotoxic activity of the compound was analyzed at the same concentration on MCF-10A and 3T3-L1 cell (considered as non-cancerous cells), no cytotoxic activity was observed (Figs. 2g-i). These data showed that the compounds of the series **6** exhibited a high selective cytotoxic activity against cancerous cells.

The calculation of the inhibitory concentration (IC_{50}) of the compounds showed that both breast cancer cell lines were sensitive to the compounds (Table 2), independently of the subtype of breast cancer MCF-7 (ER+, PR+ and HER2+) or MDA-MB-231 (ER-, PR- and HER2-). Of course, the compound **6a** appeared most potent, it is important to mention that **6f** and **6c** also showed an IC_{50} activity that could be considered clinically acceptable. A structure-activity relationship showed that the substitution of oxindole-ring-nitrogen with diphenylacetyl group decreases the cytotoxic activity. It can be inferred that that free N-H in oxindole ring is a key group in the cytotoxic affect. Furthermore, it is suggested that substituents on azetidinone ring have role in enhancing the cytotoxic activity.

***In silico* analysis**

The prediction values of the ΔG_b of series **5a-f** and **6a-f** docked in the DMD2 protein showed in site s1 records lower (range: from −7.6 to −9.9 Kcal/mol) than site s2 (range: from −4.0 to −5.1 Kcal/mol) and inhibition constant (K_i) in the series **6a-f** showed records higher than series **5a-f** in both sites. It can be observed that series **5a-f** shows better results than series **6a-f**. However, only series 6 lacked cytotoxic activity, compounds **6a**, **6e** and **6f** are of particular interest despite presenting a predicted K_i results (-7.6, -7.7 and 7.9 µM, respectively) that are high compared with Ki recorded to 6SS and 4SS (0.06 and 0.1 µM, respectively).

The analysis of interactions between the amino acids and ligands **6SS** and **4SS** on the active site s1 (Table 6) showed that ligand **6SS**, a spiro-oxindole derivative had interactions with seven aminoacids (Leu54, Leu57, Ile61, Tyr67, Phe91, Val93 and Ile99). Previous biological results showed that compound **6a** had the best cytotoxic effect and we can see that this ligand has the same interactions as ligand **6SS**. It is, therefore, suggested that the free NH group is key in the biological activity; therefore, as compared interaction between compounds **5a** and **6a** was done, results showed in Table 4. A 3D structure of typical models obtained in Docking are showed in Fig. 5. Results indicate that binding pattern from compound 6a is closed like occurred in 6SS, binding site interaction s1 of MDM2 protein in complex with compound **6a** is displayed in Fig. 5 C.

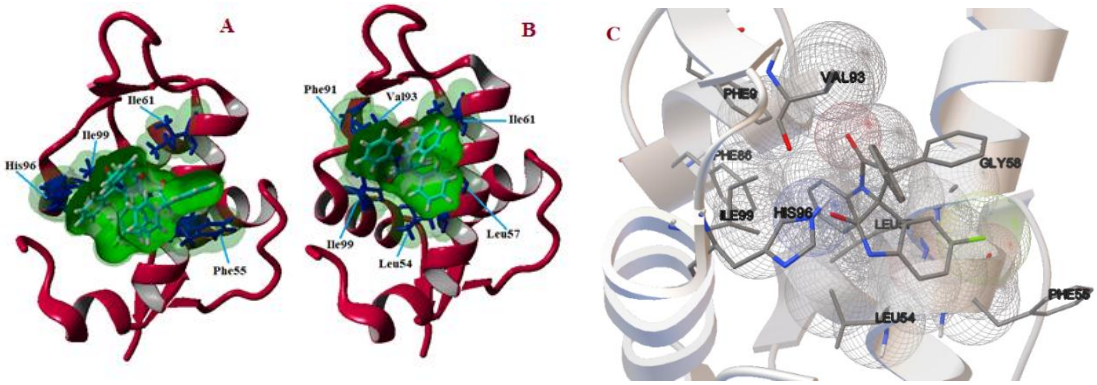

Fig. 5. Structure of the MDM2–5a (A) and MDM2–6a (B) complex. Binding site interaction s1 to MDM2-6a complex (C).

The principal interaction in the s1 binding is hydrophobic interaction especially in 4SS and 6SS as well as in both series docked; we found halogen bond in 6SS, 6c and 6e compounds. Also, the binding in s1 arise through π-stacking interactions between series 5a-f compounds and Tyr67 (Table 4) and in the case of series 6a-f compounds there are π-stacking or π-cation interactions with His96 (Table 4). This notorious difference perhaps has significance in the understanding of MDM2–p53 and their inhibitors. We found in site s2 that both series of compounds had their binding by hydrophobic interaction and hydrogen bond, these results are not conclusive in how these interaction are related to the functionality of the MDM2 protein. So, in despite recording in site 2 a low K_i prediction (range from 0.25 to 1.2 mM) the possibility of causing an effect on the union in the union site is not ruled out.

CONCLUSION

In conclusion, the paper describes the synthesis and characterization of twelve new spirooxindoles that can be of potential biological interest. The compounds from series **6a-6f** showed anticancer activity. In particular, compound **6a** showed a high anticancer activity on MDA-MB-231 and MCF-7 cell lines and a low toxicity on non-cancerous cells lines. Therefore, this compound may be useful in design of new and more potent analogues to treat breast cancer. Additionally, Docking analysis revealed that compound 6a is a potential MDM2 inhibitor, compound 6a recorded relevant interactions in Leu54, Leu57, Ile61, Phe91, Val93 and Ile99, and is predicted to be of moderate affinity; both results are encouraging to continue with research on the design of new inhibitors.

CONFLICT OF INTEREST

The authors confirm that this article content has no conflict of interest.

ACKNOWLEDGEMENTS

We wish to express our gratitude to the SIP-IPN for their financial support (20170207). Gildardo Rivera hold a scholarship from the “Comisión de Operación y Fomento de Actividades Académicas” (COFAA-IPN) and the “Programa de Estímulos al Desempeño de los Investigadores” (EDI-IPN). Francisco Reyes-Espinosa thanks to CONACYT for the scholarship 204984.

REFERENCES

1. Singh GS, Desta ZY. Isatins as privileged molecules in design and synthesis of spiro-fused cyclic frameworks. Chem Rev, 2012; 112: 6104-6155.
2. Santos MMM. Recent advances in the synthesis of biologically relevant spirooxindoles, Tetrahedron, 2014; 70: 9735-57.
3. Badillo JJ, Hanhan NV, Franz AK. Enantioselective synthesis of substituted oxindoles and spirooxindoles. Curr Opin Drug Discov Devel, 2010; 13: 758-776.
4. Yu B, Yu Q, Liu HM. Spirooxindoles: Promising scaffolds for anticancer agents. Eur J Med Chem, 2015; 97: 673-98.
5. Nayak SK, Khatik GL, Narang R, Monga V, Chopra HK. p53-Mdm2 interaction inhibitors as novel nongenotoxic anticancer agents. Curr Cancer Drug Targets, 2018; 18: 749-772.
6. Singh GS. β-Lactams in the new mellenium-Part-I. Mini-Rev Med Chem, 2004; 4: 69-92.
7. Singh GS. Sudheesh, S. Advances in synthesis of monocyclic β-lactams. Arkivoc, 2014; i: 337-385.
8. Rosenblum SB, Huynh T, Afonso A, Davies Jr HR, Yumibe N, Cladder JW, Burnett DA. Design of 1-(4-fluorophenyl)-(3R)-[3-(4-fluorophenyl)-(3S)-hydroxypropyl]-(4S)-(4-hydroxyphenyl)-2-azetisinone (SCH58235): A designed, potent, orally active inhibitor of cholesterol absorption. J Med Chem, 1998; 41: 973-980.
9. Balderas-Renteria I, Gonzalez-Barranco P, Garcia A, Banik BK, Rivera G. Anticancer drug design using scaffolds of β-lactams, sulphonamides, quinolones, quinoxalines, and natural products. Drugs advances in clinical trials. Curr Med Chem, 2012; 19: 4377-4398.
10. Singh GS, Al-Kahraman YMSA, Mpadi D, Yasinzai M. Synthesis, antimicrobial, and brine shrimps lethality assays of 3,3-diaryl-4-(1-methyl-1H-indol-3-yl)azetidin-2-ones, J Heterocycl Chem, 2015; 52: 614-619.
11. Singh GS, Al-Kahraman YMSA, Mpadi D, Yasinzai M. Synthesis of N-(1-methyl-1H-indol-3-yl)methyleneamines and 3,3-diaryl-4-(1-methyl-1H-indol-3-yl)azetidin-2-ones as potential antileishmanial agents, Bioorg Med Chem Lett, 2012; 22: 5704-5706.
12. Piccirilli RM, Popp FD. The reaction of isatin with cycloalkylamines. J Heterocycl Chem, 1973; 10: 671-673.
13. Ibata T, Singh GS. Formation of diazoketones and azines by improved oxidation of ketohydrazones using $Cu(acac)_2$ as catalyst. Tetrahedron Lett, 1994; 35: 2481-2484.
14. Nenitzescu CD, Solomonica E. Preparation of benzil monohydrazone and azibenzil, Org Synth, 1950; Coll. Vol. II: 496.
15. Singh GS. Synthesis of novel spiroazetidinones by selective lactam – carbonyl cleavage in 1-aryl/cyclohexyl-3,3-diphenyl-1'-(diphenylacyl)-2-oxospiro[azetidin-4,3'-indolin-2'-ones] using sodium hydroxide, J Heterocycl Chem, 2000; 37: 1355-1356.
16. Mosmann T. Rapid colorimetric assay for cellular growth and survival: Application to proliferation and cytotoxicity assays. J Immunol Methods, 1983, 65, 55-63.
17. Berman HM, Westbrook J, Feng Z., Gilliland G., Bhat TN, Weissig H, Shindyalov IN, Bourne PE. The Protein Data Bank Nucleic Acids Res, 2000; 28: 235-242.

18. Krieger E, Joo K, Lee J, Raman S, Thompson J, Tyka., Baker D, Karplus K. Improving physical realism, stereochemistry, and side-chain accuracy in homology modeling: Four approaches that performed well in CASP8. Proteins, 2009; 77: Suppl. 9: 114-22.
19. Laskowski RA, Swindells MB. LigPlot+: multiple ligand–protein interaction diagrams for drug discovery. J Chem Inf Model, 2011; 51: 2778-2786.
20. Morris GM, Huey R, Lindstrom W, Sanner MF, Belew RK, Goodsell DS, Olson AJ. Autodock4 and AutoDockTools4: automated docking with selective receptor flexibility. J Comput Chem, 2009; 16: 2785-91.
21. Volkamer A, Kuhn D, Grombacher T, Rippmann F, Rarey M. Combining global and local measures for structure-based druggability predictions. J Chem Inf Model, 2012; 52: 360-372.